research papers

Recent developments in microdiffraction on protein crystals

Christian Riekel

European Synchrotron Radiation Facility, B.P.220, F-38043 Grenoble Cedex, France

Protein crystallography microdiffraction and micro small-angle X-ray scattering at a 3rd generation synchrotron radiation source undulator beamline both require a compromise on beam size and beam divergence. Micro small-angle X-ray scattering requires in addition an as close as possible angular approach to the direct beam, which is mainly limited by the beam divergence at the sample position. Both techniques have been developed at the ESRF microfocus beamline in a complimentary way. The development of a dedicated microgoniometer in the frame of an EMBL/ESRF collaboration has revealed the potential of microdiffraction for protein crystallography and is a step in the quest for user friendly instrumentation.

Keywords: synchrotron radiation microdiffraction.

1. Introduction

The aim of X-ray microdiffraction (micro-XRD) on protein crystals is to investigate crystals, which cannot be grown sufficiently large for standard data collection. Micro-XRD on proteins has to address the issues of weakly scattering and radiation sensitive samples. In order to limit radiation damage, background scattering from the optical system and the sample environment has to be reduced as far as possible. Providing a microbeam of a size equal or smaller than a flash-frozen crystal allows minimizing the scattering background from the cryoprotectant. Beam defining techniques well known in small-angle X-ray scattering (SAXS) allow in addition reducing scattering from the optical system. In the present text we will discuss several topics, which have led to the development of a dedicated microgoniometer at the microfocus beamline (ID13) of the European Synchrotron Radiation Facility (ESRF) in collaboration with EMBL-Grenoble outstation. Although the issue of radiation damage is important (Henderson 1990; Perrakis et al., 1999; Glaeser et al., 2000) this topic will not be considered below as experience has shown large fluctuations in radiation sensitivity for a variety of crystals. The most sensitive protein crystals studied by micro-XRD start to die after a single shot while other can be kept in the beam for complete data collection. An important issue for the microgoniometer is therefore the possibility of examining rapidly several crystals from the same batch or to map within a crystal in order to collect sufficient data.

## 2. Instrumental issues

2.1. Resolution and background

The large unit cells of proteins require a high order resolution Δs, which is also a prerequisite for SAXS. The Δs-resolution is determined by the convolution of source/optics and detector terms (Riekel et al., 1996):

$$\Delta s = [(\Delta\alpha/\lambda)^2 + (\Delta\alpha_d/\lambda)^2]^{0.5} \qquad (1)$$

$\Delta\alpha/\lambda$ is the contribution from source and optics ($\Delta\alpha$: divergence; λ: wavelength) (Fig. 1A). The detectors term $\Delta\alpha_d/\lambda$ is defined by:

$$\Delta\alpha_d/\lambda = [(b^2 + PSF^2)/L_D]^{0.5} \qquad (2)$$

b is the size of the beam on the detector, PSF the detector point-spread-function and L_D the distance sample-to-detector. For the ID13 beamline a factor 10 demagnifying ellipsoidal mirror results in a divergence of $2.0_{hor} \times 0.2_{vert}$ mrad (Riekel 2000). A collimating slit system is used to further reduce the horizontal divergence.
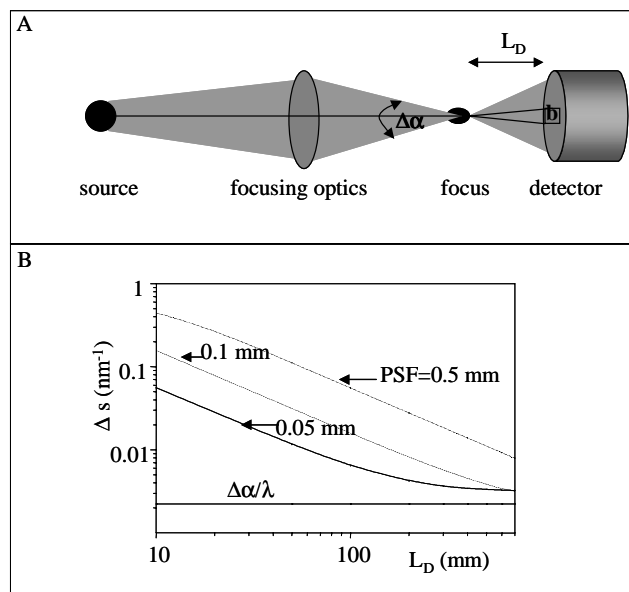

Figure 1 A: schematic design of focusing X-ray optical system; a 2D-detector is placed at a variable distance L_D from the focus. B: calculation of order resolution Δs for different detector point-spread-function values (PSF) and as a function of L_D.

Fig. 1B shows the influence of the PSF on Δs as a function of L_D (simulation parameters: $\Delta\alpha$=0.2 mrad, 10 μm beam, λ=0.095 nm). CCD detection systems with PSF≈100 μm are readily available. A smaller PSF-value would allow reducing L_D for an equivalent Δs and therefore to build a more compact beamline. Compactness is an important issue as it allows scaling down the path of the beam between the collimating system and the beamstop and hence the background scattering from air. For SAXS-applications the closest angular approach to the direct beam is also of importance (Q_{min}). In practice a pinhole collimating system with a defining aperture and a guard apertures is used in order to reduce stray radiation at the origin. For micro-SAXS applications electron microscopy apertures down to 5 μm diameter are currently used (Riekel et al., 2000). In order to be able neglecting the detector contribution to Q_{min}, a small PSF is again required (Riekel et al., 2000). For a 5 μm diameter beam, a PSF of ≈100 mm and a distance sample-to-detector of a few 100 mm one can resolve an about 100 nm peak from the beamstop.

2.2. Microgoniometer development

Single crystal micro-XRD started at ID13 with the construction of a vacuum goniometer for the study of inorganic crystals such as CaF_2. The aim was to study sub-μm^3 sample volumes in order to obtain extinction free data and hence accurate electron density maps (Rieck & Schulz, 1991).
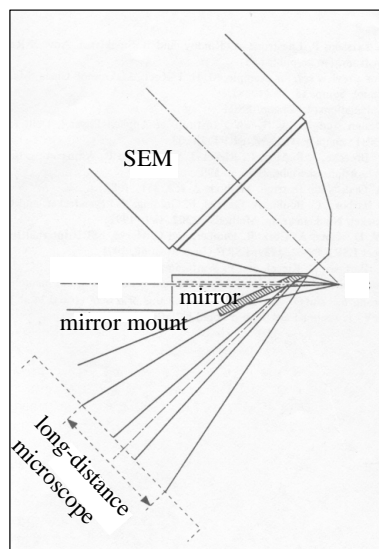
Figure 2 Conceptual study of sample environment for a vacuum goniometer. The pierced mirror mount/mirror allows observing the sample by a long-distance microscope and the X-ray beam to pass. The microgoniometer is not shown.

Fig. 2 shows a design study of the sample stage of a vacuum goniometer (Riekel et al., 1992). For sample observation a long distance optical microscope and a scanning electron microscope (SEM) head were envisaged. The SEM was introduced to image micro-crystals, which were too small to be observable by an optical microscope. A pierced mirror/mirror-mount allows both the X-ray beam to pass and the sample to be observed by the optical microscope couple to a video camera. The SEM option was not pursued due to the anticipated difficulty in stabilizing the electron beam near a motorized rotating axis. A Nonius K-goniometer with vacuum capability and 5 μm sphere of confusion (SOC) served, however, to solve a number of small unit cell crystal structures (Neder et al., 1996; Burghammer, 1997; Fiedler, 1997; Pluth et al., 1997; Broach et al., 1999; Neder et al., 1999). The vacuum capability was, however, only rarely used (Burghammer, 1997), principally due to a rapidly growing interest in organic (Madsen et al., 1999) and in particular protein micro-crystals, which required cryoflow conditions (Luger et al., 1997; Pebay-Peyroula et al., 1997; Berthet-Colominas et al., 1999). The necessity of manual centering of crystals using goniometer heads and the fact that X-ray beam and the observation direction of the long-distance microscope were not coaxial resulted in rather long alignment times for individual crystals. This led to the development of a user-friendly single rotation axis goniometer as a common project between EMBL Grenoble-outstation and ESRF (Cusack et al., 1998; Perrakis et al., 1999). The sample environment of this micro-goniometer (Fig. 3) shows several features, which have been discussed above.

Thus a pierced objective lens combined with a video camera allows to optically observe the sample but also to pass the X-ray beam. The beam is observed in-situ on a fluorescent screen and a selected position of the sample can be moved semi-automatically into the beam position. For particularly radiation sensitive samples or special sample geometries (e.g. needles) the sample can be mapped through the beam and patterns recorded for a rotational increment at every step. Electron microscopy apertures of 5/10/30 μm define the beam size. A 100 μm diameter guard aperture is placed at the end of a background reducing metal capillary at a fixed

distance of about 27 mm to the defining aperture. Although this system represents an advance in terms of background reduction, it does not allow obtaining an optimum Q_{min} for micro-SAXS applications as the distance of the two apertures is fixed and the second aperture cannot be matched to the first (see above).
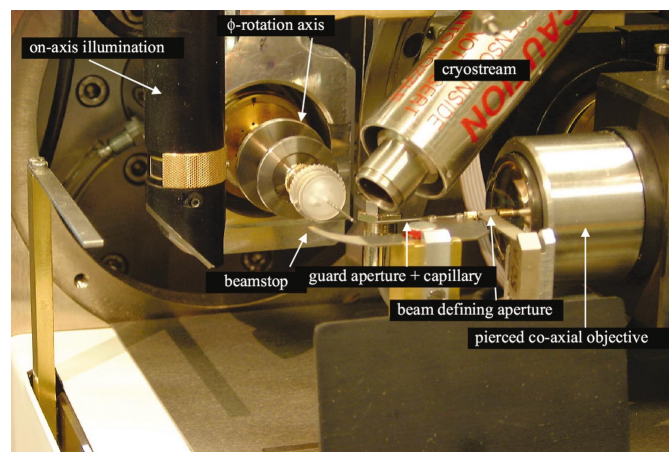

Figure 3 Image of sample environment of microgoniometer. (Courtesy of F. Cipriani, Grenoble.)
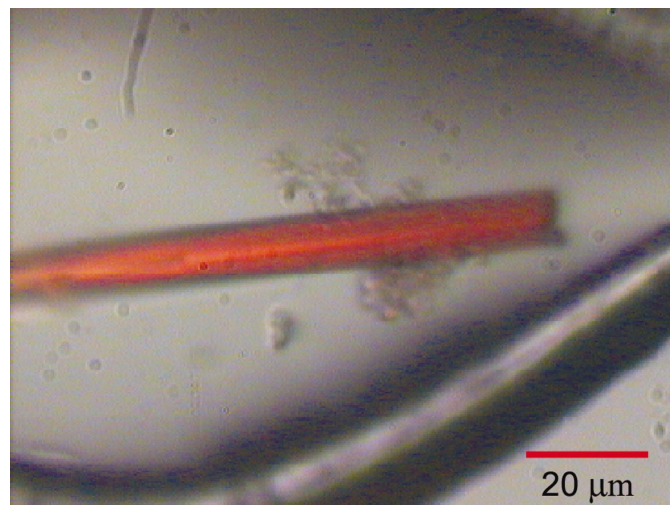
Figure 4 Cryocooled crystal of trigonal bovine rhodopsin within nylon loop as visualized on the microgoniometer. (Courtesy of G. Schertler, Cambridge.)

Fig. 4 shows a crystal of the trigonal modification of native bovine rhodopsin (P3$_1$; a=10.38 nm, c=7.66 nm), which is one of the smallest, and highly radiation sensitive crystals studied until now. (Edwards et al., 2003) Data collection is limited to a few shots at a specific location for a flux density of about 10^9 ph/sec/μm^2/100mA, which requires mapping the crystal combined with rotation. The currently attained resolution limit of about 0.265 nm required optimizing the crystallization conditions from detergent solution for about 2 years. A typical diffraction pattern is shown in Fig. 5. As the crystal quality could virtually only be studied with a microbeam, the importance of establishing long-term collaborations for such difficult crystallization projects is obvious. It is also interesting to note that the number of short measuring periods for crystal testing (1-2 shifts) is quite high at ID13.
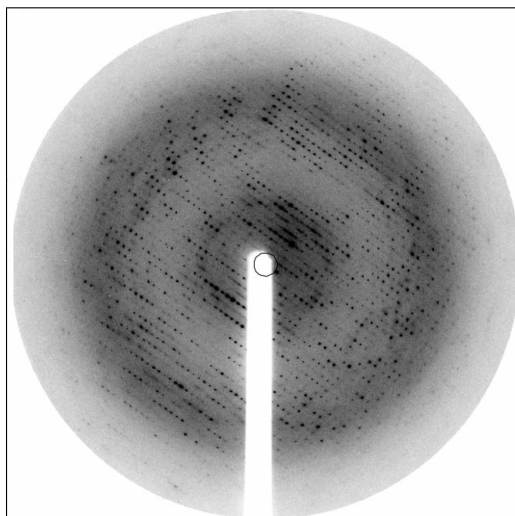
Figure 5 Diffraction pattern of trigonal bovine rhodopsin at 110 K. (Edwards et al., 2003) (λ = 0.0782 nm, 10 µm beam – 1° rotation, MAR-CCD, 20 s/exposure).

3. Outlook

The first generation microgoniometer is routinely used at ID13 for protein crystallography applications and a commercial version is now available. (MAATEL S.A.) Further automation by a sample transfer robot or automatic crystal centering is underway (Cipriani, 2003). The use of scanning diffractometry (Riekel, 2000) for mapping polymer and biopolymer samples is standard practice using a special scanning set-up (Riekel, 2000). This technique is also used with the microgoniometer for selecting small unit-cell micro-crystals within a powder-batch for data collection and could also be applied to protein crystallography, provided that the radiation damage is kept at a low level. The smallest protein crystal sizes currently accessible to full data collection are in the range of about 10 µm. It will be interesting to explore whether a further reduction in crystal volume is possible for particularly radiation resistant systems. This will require optimising the S/N ratio as far as possible by reducing instrumental background, background from the sample environment and using He-cryoflow conditions.

Reducing the beam size to the subµm range will provide more freedom for mapping experiments. Subµm X-ray beams can be generated by Kirkpatrick-Baez mirrors (Hignette et al., 2001), Fresnel zone plates (David et al., 2002) or refractive lenses (Schroer et al., 2003). The choice of a specific optics will depend on the background noise level and a sufficiently high order resolution. A complimentary development is to generate low divergence microbeams of a few microns diameter by long focal-length refractive lenses combined with defining apertures in order to increase the order resolution (see above) (Burghammer et al., 2003).

References

Berthet-Colominas, C., Monaco, S. Novelli, Sibai, G., Mallet, F. & Cusack, S. (1999). *The EMBO Journal,* **18**, 1124-1136.
Broach, R. W., Bedard, R. L., Song, S.G., Pluth, J.J., Bram, A., Riekel, C. & Weber, H.P. (1999). *Chemistry of Materials,* **11**, 2076-2080.
Burghammer, M. (1997). PhD-thesis, University of Munich, Germany.
Burghammer, M., Kuhlmann, M., Lengeler, B., Riekel, C., Roth, S., Schroer, C., Snigirev, A. & Snigireva, I. (2003). Personal communication.
Cipriani, F. (2003). Personal communication.
Cusack, S., Belrhali, H., Bram, A., Burghammer, M., Perrakis, A. & Riekel, C. (1998). *Nature Structural Biology,* **5**, 634-637.
David, C., Noehammer, B. & Ziegler, E. (2002). *Microelectronic Engineering,* **61-62**, 987-992.
Edwards, P., Li, J., Burghammer, M., McDowell, J.H., Villa, C., Hargrave, P. & Schertler, G.F.X. (2003). Personal communication.
Fiedler, S.M. (1997). PhD-thesis, University Frankfurt/Main, Germany.
Glaeser, R., Facciotti, M., Walian, P., Rouhani, S., Holton, J., MacDowell, A., Celestre, R., Cambie, D. & Padmore, H. (2000). *Biophysical Journal,* **78**, 3178-3185.
Henderson, R. (1990). *Proc. Roy. Soc. B.* **241**, 6-8.
Hignette, O., Rostaing, G., Cloetens, P., Rommeveaux, A., Ludwig, W. & Freund, A. (2001). *Proc. SPIE,* **4499,** 105-116.
Luger, K., Maeder, A.W., Richmond, R.K., Sargent, D.F. & Richmond, T.J. (1997). *Nature* **389**, 251-260.
Madsen, D., Burghammer, M., Fiedler, S. & Müller, H. (1999). *Acta Cryst.* **B55**, 601-606.
Neder, R. B., Burghammer, M., Grasl, T.H., Schulz, H., Bram, A., Fiedler, S. & Riekel, C. (1996). *Zeitschrift f. Kristallographie,* **211**, 763-765.
Neder, R. B., Burghammer, M., Grasl, T.H., Schulz, H., Bram, A. & Fiedler, S. (1999). *Clays and Clay Minerals,* **47**, 487-494.
Pebay-Peyroula, E., Rummel, G., Rosenbusch, J.P. & Landau, E.M. (1997). *Science,* **277**, 1676-1681.
Perrakis, A., Cipriani, F., Castagna, J.C., Claustre, L., Burghammer, M., Riekel, C. & Cusack, S. (1999). *Acta Cryst.* **D55**, 1765-1770.
Pluth, J. J., Smith, J. V. Pushcharovsky, D.Y., Semenov, E.I., Bram, A., Riekel, C., Weber, H.P. & Broach, R.W. (1997). *Proc Nat Acad Sci.* **94**, 12263-12267.
Rieck, W. & Schulz, H. (1991). *Handbook of Synchrotron Radiation,* Vol.3, edited by G. Brown and D. E. Moncton, pp. 267-290. New York: Elsevier
Riekel, C. (2000). *Rep. Prog. Phys.* **63**, 233-262.
Riekel, C., Bösecke, P., Diat, O. & Engström, P. (1996). *Journal of Molecular Structure,* **383**, 291-302.
Riekel, C., Bösecke, P. & Sanchez del Rio, M. (1992). *Rev. Sci. Instrum.* **63**, 974-981.
Riekel, C., Burghammer, M. & Müller, M. (2000). *J. Appl. Cryst.* **33**, 421-423.
Schroer, C. G., Kuhlmann, M., Hunger, U.T., Gunzler, T.F., Kurapova, O., Feste, S., Frehse, S., Lengeler, B., Drakopoulos, M., Somogyi, A., Simionovici, A.S., Snigirev, A., Snigireva, I., Schug, C. & Schroder, W.H. (2003). Appl. Phys. Letters, 82, 1485-1487.